

Ag Functionalized Molybdenum Disulfide Hybrid Nanostructures for Selective and Sensitive Amperometric Hydrogen Peroxide Detection

Zhenting Zhao¹, Jie Liu², Wenda Wang², Jun Zhang², Gang Li², Jianqi Liu¹, Kun Lian², Jie Hu^{2,*}, Serge Zhuiykov^{3,*}

¹ School of Information Engineering, Guangdong Mechanical & Electrical College, Guangzhou 510515, Guangdong, China

² Micro and Nano System Research Center, Key Lab of Advanced Transducers and Intelligent Control System (Ministry of Education) & College of Information Engineering, Taiyuan University of Technology, Taiyuan 030024, Shanxi, China

³ Ghent University Global Campus, Department of Applied Analytical & Physical Chemistry, Faculty of Bioscience Engineering, 119 Songdomunhwa-ro, Yeonsu-gu, Incheon 21985, South Korea

*E-mail: hujie@tyut.edu.cn, serge.zhuiykov@ghent.ac.kr

Received: 6 May 2017 / Accepted: 24 July 2017 / Published: 13 August 2017

Ag nanoparticles functionalized flower-like molybdenum disulfide (MoS₂) hybrid nanostructures (AgNPs/MoS₂) were successfully synthesized by a facile hydrothermal method. The structure and surface morphology were subsequently characterized by scanning electron microscopy (SEM), transmission electron microscopy (TEM), X-ray diffraction (XRD) and X-ray photoelectron spectroscopy (XPS) techniques. The as-synthesized AgNPs/MoS₂ hybrid nanostructures were modified on a glassy carbon electrode (GCE) and further utilized for amperometric hydrogen peroxide (H₂O₂) detection. The electrochemical behaviors and sensing performance of the AgNPs/MoS₂/GCE were studied by cyclic voltammetry (CV) and single-potential amperometry methods. The obtained results have demonstrated that the developed AgNPs/MoS₂/GCE amperometric sensor possesses an excellent catalytic performance toward the reduction of H₂O₂. The as-prepared electrochemical sensor exhibits fast response time of less than 3 s, large linear detection range of 0.025-135.2 mM ($R^2=0.998$) and high sensitivity of 54.5 $\mu\text{A}\cdot\text{mM}^{-1}\cdot\text{cm}^{-2}$. Moreover, the developed H₂O₂ sensor has shown good anti-interference ability, outstanding stability and reproducibility, which represents a great potential for H₂O₂ detection in practical applications.

Keywords: Molybdenum disulfide, Silver nanoparticles, Hydrogen peroxide, Electrochemical sensor

1. INTRODUCTION

Hydrogen peroxide (H_2O_2), a strong oxidizing agent and essential intermediate [1], is easily immiscible with water. It has been extensively utilized in the food processing, biomedical science and pharmaceutical engineering [2]. Therefore, H_2O_2 is an important target analyte, requiring precise, sensitive, quantitative and selective analysis in the fields of food security, environmental protection and bioanalysis [3-5]. So far various measurement methods have been utilized for the accurate detection of H_2O_2 [6-8]. Among them the electrochemical technology has been considered to be the most promising because of its excellent advantages including rapid response, convenient operation and high sensitivity [9-11]. Usually, the non-enzymatic and enzymatic H_2O_2 electrochemical sensors are the most commonly used types. Previous works have demonstrated that the non-enzymatic sensor can well avoid the disadvantages of instability and poor reproducibility, providing an effective way for H_2O_2 determination [12-14].

Nevertheless, the rapid development of nanoscience and nanotechnology has discovered new kinds of nanomaterials capable of catalyzing reduction of H_2O_2 . Thus, they could be successfully employed in the non-enzymatic H_2O_2 sensors. Inspiringly, noble metal nanoparticles have played important role in the construction of non-enzymatic H_2O_2 electrochemical biosensors owing to their unique and unmatched electro-catalytic properties, specific surface area and wonderful electron transfer ability [15-17]. Among these noble nanometals, Ag nanoparticles (AgNPs) have been widely used for fabrication biosensors on account of its unique capabilities such as biocompatibility, low toxicity and intriguing catalytic activity [18-20]. However, strong van der Waals force could cause aggregation between AgNPs, resulting in the sensor's performance degradation. To solve this problem, various support materials, for example, graphene [21], poly micro-particles [22], TiO_2 [23] and carbon nanodots [24] were used for AgNPs immobilization. This approach has been confirmed to be very effective strategy in protecting AgNPs against agglomeration and improving sensing properties of the prepared sensor. In addition, molybdenum disulfide (MoS_2) owing to its large specific surface area and high chemical stability has recently been demonstrated outstanding properties suitable as an advanced support material for nanoparticles [25]. Meanwhile, recent studies have also proved that MoS_2 can be a promising candidate for electro-catalytic the H_2O_2 [26-28]. Although it seems obvious that AgNPs and MoS_2 are expected to be employed together for the development of electrochemical H_2O_2 sensors, so far little results have been reported about their combination and/or heterojunction. Therefore, for further enhancement of the electro-catalytic properties both AgNPs and MoS_2 , the AgNPs/ MoS_2 hybrid nanostructures was prepared and used for fabricating non-enzymatic H_2O_2 sensors.

In this study, flower-like MoS_2 nanostructures were synthesized by hydrothermal method. The AgNPs were distributed on the MoS_2 nanosheets by direct adsorption for the surface functionalization, which can greatly improve the properties of the developed AgNPs/ MoS_2 hybrid nanostructures for H_2O_2 sensing. The fabricated AgNPs/ MoS_2 hybrid nanostructures on modified GCE exhibited much higher current response on H_2O_2 reduction compared with AgNPs/GCE and MoS_2 /GCE. The fabricated H_2O_2 biosensors based on AgNPs/ MoS_2 hybrid nanostructures have also exhibited good stability and reproducibility.

2. EXPERIMENTAL

2.1. Reagents and characterization

Silver nitrate (AgNO_3 , > 99%), Sodium molybdate dehydrate ($\text{Na}_2\text{MoO}_4 \cdot 2\text{H}_2\text{O}$, $\geq 99.5\%$), Thiourea (NH_2CSNH_2 , $\geq 99.0\%$) and uric acid (UA, $\geq 99\%$) were purchased from Sigma-Aldrich (Shanghai, China). Ascorbic acid (AA), hydrogen peroxide (H_2O_2 , 30%) and sodium citrate were purchased from Sinopharm Chemical Reagent Co. Ltd. (Shanghai, China). All other chemicals were of analytical grade from the commercial sources and were used as received without any further purification. The double-distilled water which was used throughout the whole experiment has the resistivity of no less than $18.2 \text{ M}\Omega \cdot \text{cm}$. The 0.2 M phosphate buffer solution (PBS) was prepared by mixing solutions of Na_2HPO_4 and NaH_2PO_4 as the supporting electrolyte.

2.2. Material structure characterization

The morphologies of pristine MoS_2 and $\text{AgNPs}/\text{MoS}_2$ nanostructures were observed using scanning electron microscope (SEM, JSM-7001F) at an accelerating applied potential of 10 kV. The transmission electron microscope (TEM, JEM-2100F) was acquired to further observe the microstructures of composite with an accelerating voltage of 200 kV. The crystal structure of the as-synthesized samples were investigated by X-ray diffraction (XRD, Bruker) with a scanning speed of $3^\circ/\text{min}$. XPS measurements were performed on an Escalab 250Xi instrument with $\text{Mg-K}\alpha$ radiation. All the electrochemical measurements were carried out using IM6 electrochemical workstation (Zahner, Germany) at room temperature with a conventional three-electrode system. A bare or modified GCE was used as the working electrode, a Pt electrode was used as the counter electrode and a silver chloride electrode (saturated KCL) was used as the reference electrode for all the electrochemical measurements.

2.3. Preparation of $\text{AgNPs}/\text{MoS}_2$ hybrid nanostructures

The flower-like MoS_2 was synthesized on the basis of the previous report with a slight modification by one-step hydrothermal method [29, 30]. Specifically, 0.6 g $\text{Na}_2\text{MoO}_4 \cdot 2\text{H}_2\text{O}$ and 0.72 g NH_2CSNH_2 were dissolved into 30 mL of distilled water (DI), and the solution was stirred for 20 mins. Then the mixture solution was transferred into a 50 mL Teflon-lined autoclave and heated in 220°C for 24 h. After cooling to the room temperature naturally, the black products were washed with DI and anhydrous ethanol. Finally, the flower-like MoS_2 nanostructures were obtained by overnight drying at 60°C . The Ag nanoparticles were obtained by reducing AgNO_3 with sodium citrate [31]. 117 μL of 0.5 M AgNO_3 aqueous solution was introduced into 100 mL distilled water with 5 mL 1wt% sodium citrate aqueous solution under the stirring. Then the mixture was brought to keep on boiling for 1 h. Then Ag nanoparticles could be obtained after several times washing, certification and drying.

The $\text{AgNPs}/\text{MoS}_2$ hybrid nanostructures were prepared by direct adsorption of the as-developed AgNPs onto flower-like MoS_2 . The hybrid nanostructures were prepared as follows: 1 ml of

MoS₂ aqueous solution (2 mg/mL) was mixed with 1 ml of AgNPs aqueous solution (29.25mM/L), and then the mixture was sonicated for at least 1 h. The mixture was placed over one night at the room temperature. Finally, the resulting AgNPs/MoS₂ hybrid nanostructures were obtained by centrifugation and dispersed into 1 ml of anhydrous ethanol for the future use.

2.4. Fabrication of the H₂O₂ electrochemical sensor

The modified sensor electrodes were fabricated by the simple casting method. Firstly, a GCE was polished repeatedly with 0.3 μm and 0.05 μm alumina powder. Secondly, the GCE was cleaned by successive sonication in distilled water, ethanol and distilled water for 5 min and dried in air. Then the AgNPs/MoS₂ hybrid solution was ultra-sonicated for 30 min to form a homogeneous suspension. After that, 10 μL of AgNPs/MoS₂ suspension was dropped onto the cleaned GCE and dried at 60 °C to develop a uniform film on the electrode surface. The obtained modified sensing electrode was defined as AgNPs/MoS₂/GCE. Finally, after washing with distilled water the AgNPs/MoS₂/GCE was used for electrochemical H₂O₂ detection. In addition, both AgNPs/GCE and MoS₂/GCE electrodes were prepared for comparative measurements using similar procedure. All of the fabricated and modified electrodes were stored at 4 °C when they were not used.

3. RESULTS AND DISCUSSION

3.1. Characterization of the nanostructures

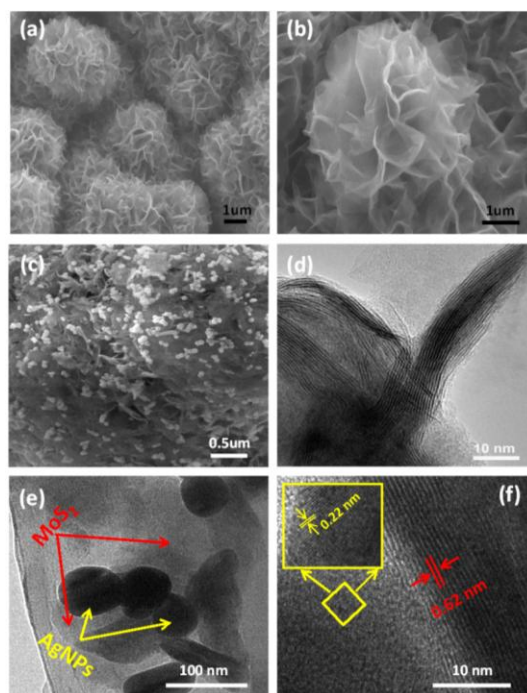


Figure 1. SEM images of the pristine MoS₂ in low (a) and high magnification (b); SEM image of AgNPs/MoS₂; TEM images of the pure MoS₂ (d) and the obtained AgNPs/MoS₂ hybrid nanostructures (e and f).

Fig. 1(a-b) depicts the representative SEM images of the obtained pure flower-like MoS₂ nanostructures at different magnifications. The images show that the pristine MoS₂ nanosheets tend to stack together tightly and grow in high density, exhibiting specific flower-like nanostructure. The thickness of petal-like flakes was only several nanometers. Fig.1(c) displays the SEM image of AgNPs/MoS₂ hybrid nanostructures, where the AgNPs were scattered on the surface of MoS₂ after sonication. Fig.1(d) exhibits the HRTEM image of MoS₂, which shows that the limited-layer MoS₂ structures tended to stack with an interlayer distance of 0.62 nm which corresponded to the (002) plane of MoS₂. On the other hand, Fig.1 (e) presents the TEM image of AgNPs/MoS₂ hybrid nanostructures from which it is clearly visible that the AgNPs were attached onto the surface of MoS₂ nanosheets. AgNPs were about 50 nm in diameter and the shape was mostly spherical. As illustrated in Fig.1 (f), the lattice fringes with spacing of 0.22 and 0.62 nm were consistent with the spacing of the (111) planes of Ag and the (002) planes of MoS₂, respectively.

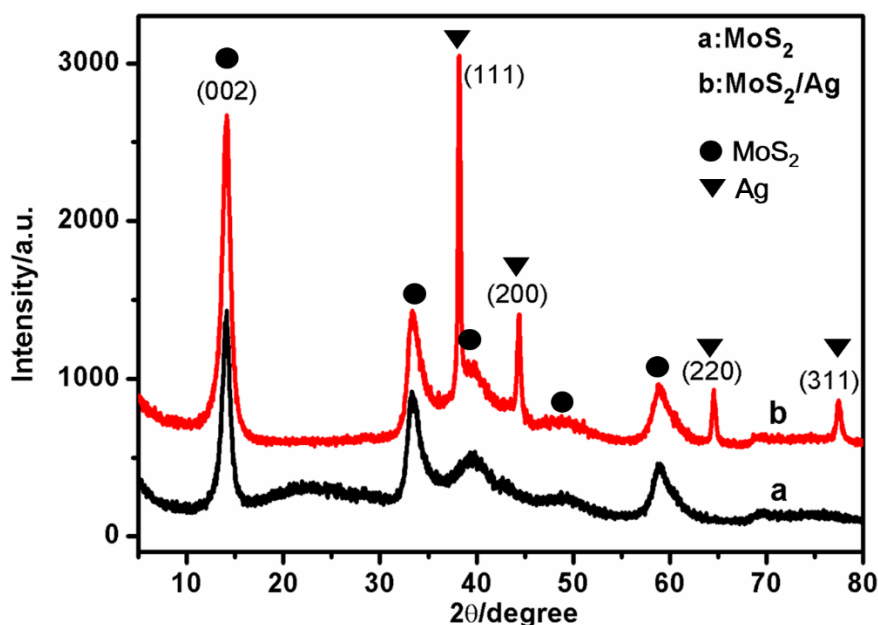


Figure 2. XRD patterns of the pure MoS₂ (trace a) and AgNPs/MoS₂ hybrid nanostructures (trace b).

The crystal structures of the as-synthesized pure MoS₂ and AgNPs/MoS₂ hybrid nanostructures samples were further investigated by XRD. Fig. 2 depicts the XRD patterns for both pure MoS₂ and AgNPs/MoS₂ hybrid nanostructures. The measured results confirmed that both pure MoS₂ and AgNPs/MoS₂ hybrid nanostructures have the diffraction peaks corresponding to the (002), (100), (103) and (110), matching the phase of MoS₂ (JCPDS 37-1492). Moreover, the prominent diffraction peaks at $2\theta = 14.1^\circ$ were corresponded to the diffraction from (002) plane of MoS₂ with the spacing of 0.62 nm. In addition, there are four more main peaks in AgNPs/MoS₂ at $2\theta = 38.2^\circ$, 44.5° , 64.5° and 77.5° , respectively, which corresponded to the (111), (200), (220) and (311) planes of the silver crystal (JCPDS No. 04-0783). These results were consistent with the TEM images, indicating the AgNPs/MoS₂ hybrid nanostructures were indeed successfully prepared by the hydrothermal method.

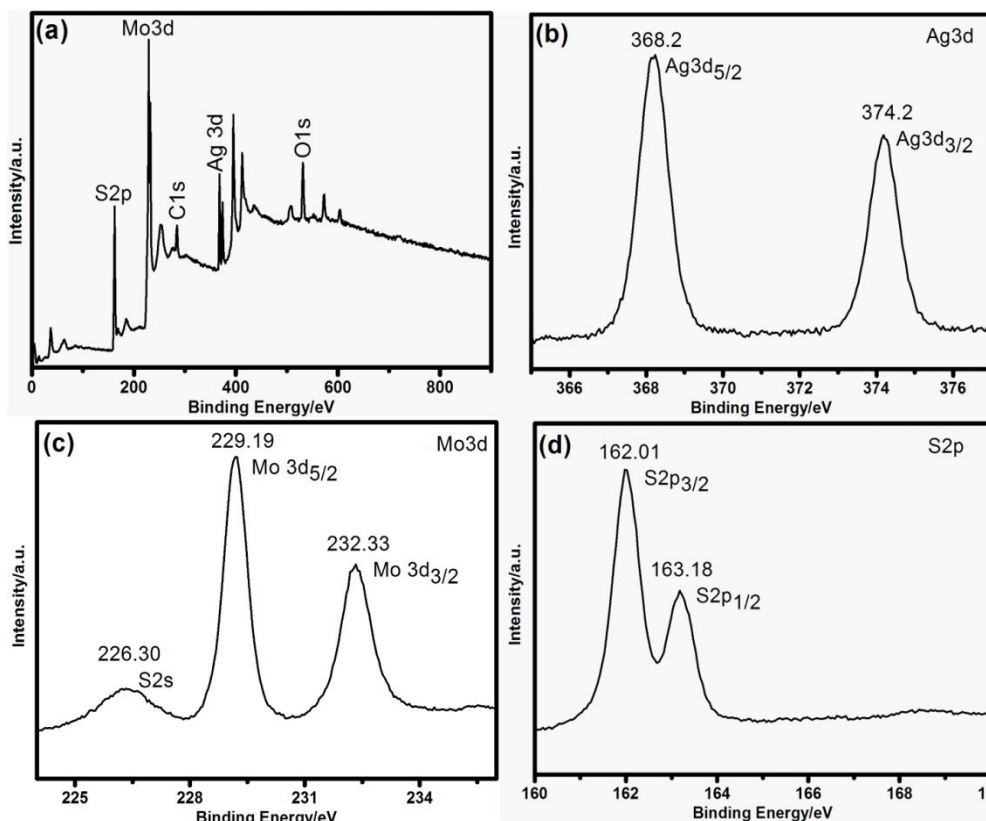


Figure 3. (a) XPS survey spectrum of AgNPs/MoS₂ composite, (b) Ag3d spectrum, (c) Mo3d spectrum and (d) S2p spectrum.

The XPS measurements were carried out on the AgNPs/MoS₂ nanocomposites to determine their elemental compositions and chemical oxidation valance state. The XPS survey spectrum is presented in Fig. 3 (a). In order to reduce the sample charging effect, the binding energies were calibrated by referencing the C 1s peak (284.6 eV). Fig. 3 (b) illustrates the high-resolution XPS peak of Ag3d, and the corresponding peaks located at 368.2 eV and 374.2 eV can be ascribed to Ag 3d_{5/2} and Ag3 d_{3/2}, respectively. Fig. 3 (c) displays the binding energies of Mo3d_{5/2} and Mo3d_{3/2}, located at 229.19 eV and 232.33 eV, which are characteristics of MoS₂. In addition, the binding energy of S2s is found at 226.3 eV, suggesting the presence of sulfur in AgNPs/MoS₂ composite. Fig. 3 (d) illustrates the S 2p spectrum, which can be convoluted into two major peaks with the binding energies at 162.01 eV and 163.18 eV, corresponding to S 2p_{3/2} and S 2p_{1/2}, respectively. Therefore, all the results obtained confirmed that Ag element exists in the as-synthesized AgNPs/MoS₂ hybrid nanomaterials.

3.2. Electrochemical H₂O₂ measurement by AgNPs/MoS₂/GCE

The electrochemical performance of the developed AgNPs/MoS₂ hybrid nanostructures were evaluated by CVs in the potential range of -0.7—0.2 V at the scan rate of 100 mV s⁻¹ (vs. Ag/AgCl). Fig. 4 (a) displays typical CVs of bare GCE, AgNPs/GCE, MoS₂/GCE, and AgNPs/MoS₂/GCE in 0.2 M PBS (pH=6.5) with 2.0 mM H₂O₂. For the bare GCE, no redox reaction peak appeared in the potential window range.

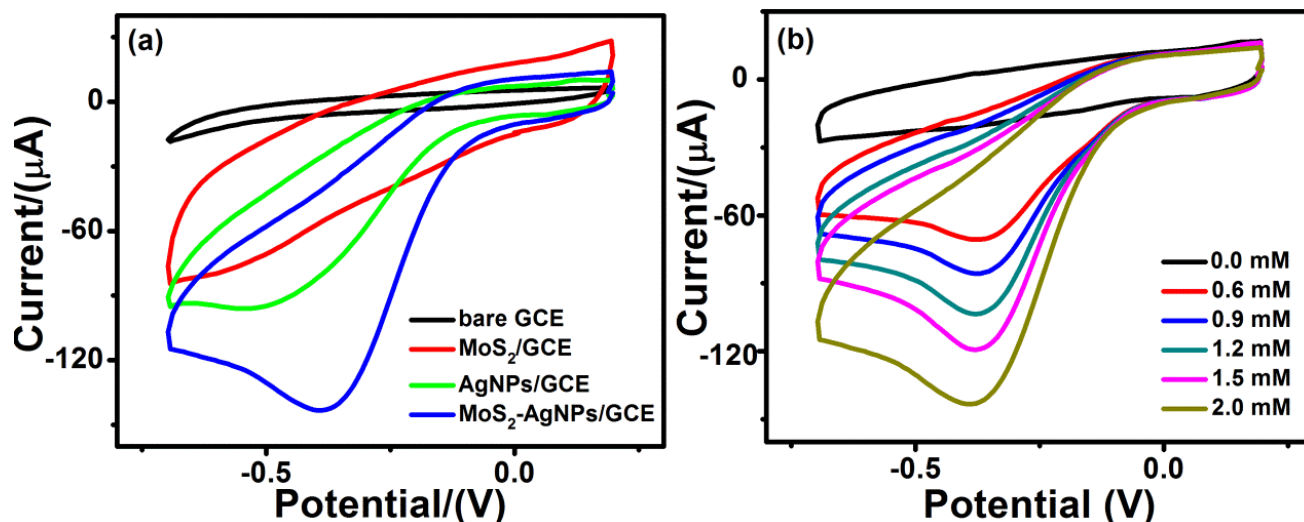


Figure 4. (a) CVs of various electrodes in N₂-saturated 0.2 M PBS (pH=6.5) in the presence of 2.0 mM H₂O₂; (b) CVs of the AgNPs/MoS₂ modified electrode in N₂-saturated 0.2 M PBS (pH=6.5) containing different concentrations of H₂O₂: 0, 0.6, 0.9, 1.2, 1.5 and 2.0 mM (scan rate: 100 mV s⁻¹).

The modified MoS₂ electrode shown a weak reduction peak response (~88.1 μA) at about -0.6 V, and a significant increased capacitive current can be observed due to its larger contact surface area. When the AgNPs was modified on the electrode, the electro-catalytic process for H₂O₂ on AgNPs/GCE achieved a reduction current peak of 96.1 μA at about -0.54 V, which is consistent with the results in previous works [32-34]. Moreover, a significantly larger reduction peak current value of 144.3 μA at the potential of -0.39 V is observed on the AgNPs/MoS₂/GCE. The more positive reduction potential and the higher catalytic current can be measured under the same concentration of H₂O₂, which indicated a better catalytic ability than the AgNPs and MoS₂. Meanwhile, the measured peak current of AgNPs/MoS₂/GCE was about 1.5 times higher than that of AgNPs/GCE, which suggested that the MoS₂ plays an important role for improving the electrochemical performance of AgNPs. Compared with the other support materials, such as CNT and rGO [34], the MoS₂ exhibits a better performance, and the AgNPs/MoS₂/GCE electrode shows a greater current response than AgNPs-CNT-rGO/GCE. Furthermore, the sensing response of AgNPs/MoS₂/GCE towards the different concentrations of H₂O₂ was also evaluated, as shown in Fig. 4 (b). It clears that the reduction peak increases with the increasing of the H₂O₂ concentration from 0 mM to 2.0 mM, which demonstrates excellent sensing performance of AgNPs/MoS₂/GCE towards H₂O₂. The measured results have unambiguously demonstrated that the AgNPs/MoS₂ hybrid nanostructures possess outstanding electro-catalytic properties for the H₂O₂ reduction, which could be used as a promising hybrid nanomaterial for fabrication of non-enzymatic H₂O₂ electrochemical sensor.

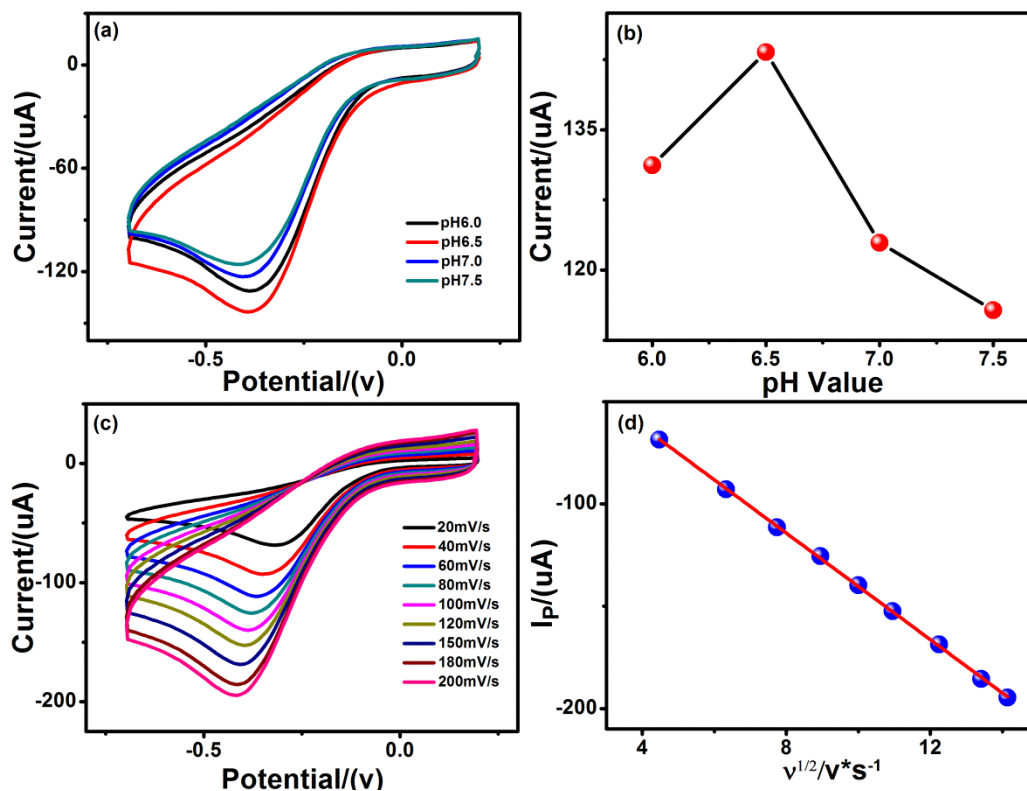


Figure 5. (a) CVs of AgNPs/MoS₂/GCE in 2.0 mM H₂O₂ buffer solution under different pH (pH=6.0, 6.5, 7.0, 7.5) with scan rate 100 mV s⁻¹; (b) the calibration curve of pH value versus peak current; (c) CVs of AgNPs/MoS₂/GCE under different scan rates (20, 40, 60, 80, 100, 120, 150, 180 and 200 mV s⁻¹) to 2.0 mM H₂O₂; (d) The calibration curve of the peak current vs. the square root of the scan rate.

The current responses of the as-prepared sensor under different pH solutions (from 6.0 to 7.5) were investigated to 2.0 mM H₂O₂, as presented in Fig. 5 (a). The measured results show that the obtained current initially increased with the increasing pH value from 6.0 to 6.5. However, further increase of pH until 7.5 caused the decrease of the current response (Fig. 5 (b)). Therefore, the phosphate buffer solution at pH 6.5 was selected as the supporting electrolyte in this work. Furthermore, the electrochemical response of AgNPs/MoS₂/GCE was also examined by performing the scan rate dependent experiments under 0.2 M PBS with 2.0 mM H₂O₂ (Fig. 5 (c)). The obtained results show that the peak current enhanced with the increasing of scan rate from 20 to 200 mVs⁻¹, and the measured correlation coefficient was about 0.999, as derived in Fig. 5(d). It demonstrates a diffusion-controlled process for the H₂O₂ reduction.

3.3. Amperometric response of the AgNPs/MoS₂ -based sensor

The sensitivity, linear response range and the detection limit are very important parameters for any electrochemical sensor. In order to investigate the electrochemical properties, the amperometric current response experiments were conducted on the developed AgNPs/MoS₂ hybrid nanostructures based H₂O₂ sensors. Fig. 6 exhibits the typical amperometric response of AgNPs/MoS₂/GCE to

introduction of H₂O₂ into 0.2 M PBS solution. It can be observed from Fig. 6 (a), that the reduction current increased sharply to reach the steady-state value within just 3 s when an aliquot of H₂O₂ was dropped into the stirring solution. Fig. 6 (b) illustrates clear linear relationship between the plateau current and the concentrations of H₂O₂. It was confirmed that the as-fabricated non-enzymatic H₂O₂ sensor has a linear response range of 0.025-135.2 mM ($R^2=0.998$) and the detection limit of H₂O₂ is estimated to be about 3.5 μ M.

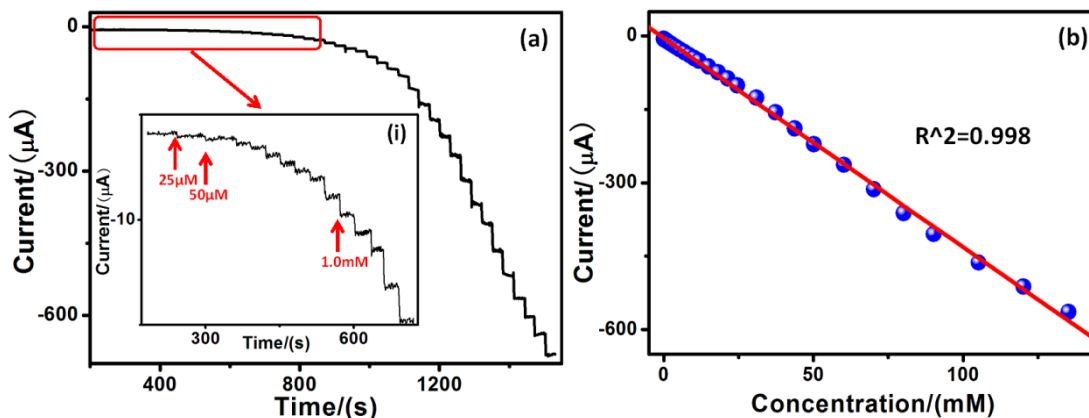


Figure 6. (a) Typical amperometric response of AgNPs/MoS₂/GCE for the H₂O₂ introduction into N₂-saturated 0.2 M PBS (pH=6.5) at the potential of -0.35 V; Inset image (i): the amplified response curve at low concentrations; (b) The linear plot of amperometric response versus H₂O₂ concentration.

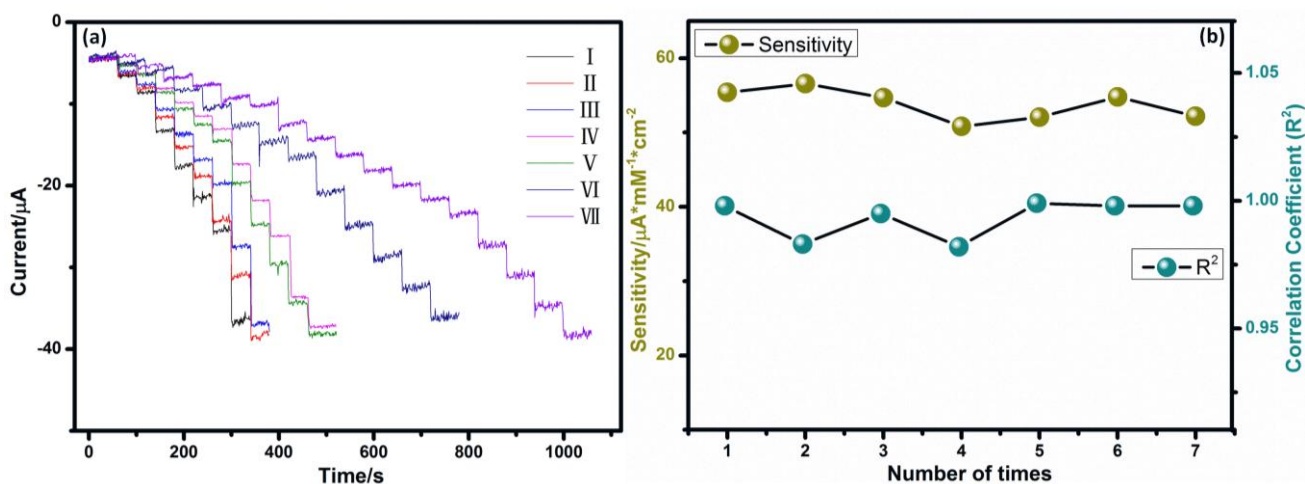


Figure 7. (a) The amperometric current response of different sensors which were fabricated by the same method for successive addition of hydrazine range from 0.3-300 μ M; (b) the calculated sensitivities of the seven results, and the correlation coefficients (R^2) of the fitting lines

The reproducibility of the sensor was evaluated by seven different amperometric experiments. Fig. 7 (a) shows the current responses of the seven experiments, and the dropping amount of the H₂O₂ is listed in Table S1 (Supplementary Information). Fig. 7 (b) presents the calculated sensitivities of the

seven amperometric experiments, and the correlation coefficients (R^2) of the fitting lines. The standard deviation of sensitivities is only about 1.9. The measured results demonstrated that the sensitivity and linearity almost remained the same, which exhibits that the fabricated sensor has excellent reproducibility.

Table 1. Comparison of AgNPs/MoS₂/GCE with various H₂O₂ sensors in previous reports.

Type of electrode	LOD (μM)	Linear range (mM)	Sensitivity	Reference
AgNPs/MWCNT/GCE	0.5	0.05-17	$1.42 \mu\text{A} \cdot \text{mM}^{-1}$	[39]
AgNPs-rGO-/ITO	5.0	0.1-100	--	[17]
PQ11-AgNPs/GCE	33.9	0.1-180	--	[31]
AgNPs/PVA/Pt	1.0	0.04-6	$128 \mu\text{A} \cdot \text{mM}^{-1}$	[35]
AgNPs-rGO/GCE	4.3	0.1-70	--	[36]
AgNPs-PMPD/GCE	4.7	0.1-30	--	[37]
AgNPs-NFs/GCE	62.0	0.1-80	--	[38]
Ag/FeOOH/GCE	15.1	0.03-11	$9.34 \mu\text{A} \cdot \text{mM}^{-1} \cdot \text{cm}^{-2}$	[40]
Al/LDH/AgNPs/CPE	6.0	0.01-10	$1.863 \mu\text{A} \cdot \text{mM}^{-1} \cdot \text{cm}^{-2}$	[41]
AgNPs-P(ABA)-Fe ₃ O ₄ /MCPE	1.74	0.005-5.5	--	[42]
AgNPs/MoS ₂ /GCE	3.5	0.025-135.2	$54.5 \mu\text{A} \cdot \text{mM}^{-1} \cdot \text{cm}^{-2}$	This work

In addition, the sensing performance of the developed AgNPs/MoS₂/GCE sensor was compared with previous reports for the H₂O₂ sensors attached with AgNPs, as shown in Table 1. The as-prepared sensor based on AgNPs/MoS₂ hybrid nanostructures have demonstrated a lower H₂O₂ detection limit (3.5 μM), larger linear response range (0.025-135.2 mM), and at the same time much higher sensitivity ($54.5 \mu\text{A} \cdot \text{mM}^{-1} \cdot \text{cm}^{-2}$). The measured results confirmed that Ag functionalized MoS₂/GCE represents successful approach towards improvement of electrochemical properties for H₂O₂ detection, which could be attributed to the unique hybrid nanostructure and synergistic effect.

3.4. Selectivity and stability of the sensor

The interference ability is an important analytical factor for an electrochemical sensor. Some co-existing interference species such as ascorbic acid (AA), uric acid (UA), glucose, NaNO₃ and NaNO₂ were found to influence the responses of a sensor for H₂O₂ detecting. Therefore, selectivity of the developed sensors based on AgNPs/MoS₂ was thoroughly investigated and the results are presented in Fig. 7. As shown in this figure, 0.05 mM H₂O₂, 1.0 mM AA, 1.0 mM UA, 1.0 mM Glucose (Glu), 1.0 mM NaNO₃, 1.0 mM NaNO₂ and 0.05 mM H₂O₂ were subsequently added into N₂-saturated 0.2 M PBS for investigating the interference ability of the AgNPs/MoS₂-based H₂O₂ sensor. The working potential was hold at -0.35 V. Another three experiments were also carried out in the same conditions, and the results were shown in Fig. S1 (Supplementary Information). The results obtained evidently confirmed excellence selectivity of the H₂O₂ sensor, as there were almost none current responses to the

introduction of the interference agents. Thus, all these interferences have provided little to none impact on the H₂O₂ detection in current conditions.

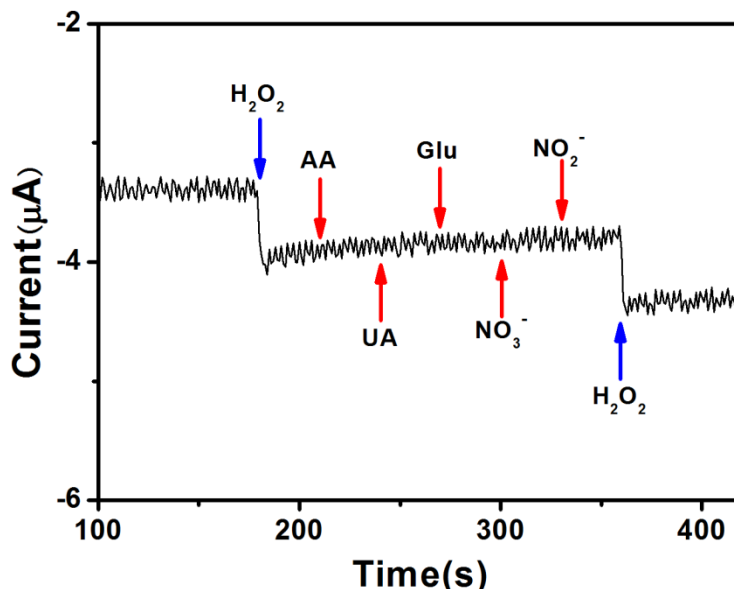


Figure 8. Interference study with the successive addition of 0.05 mM H₂O₂, 1.0 mM AA, 1.0 mM UA, 1.0 mM Glucose (Glu), 1.0 mM NO₃⁻, 1.0 mM NO₂⁻ and 0.05 mM H₂O₂ into a stirred N₂-saturated 0.2 M PBS (pH=6.5).

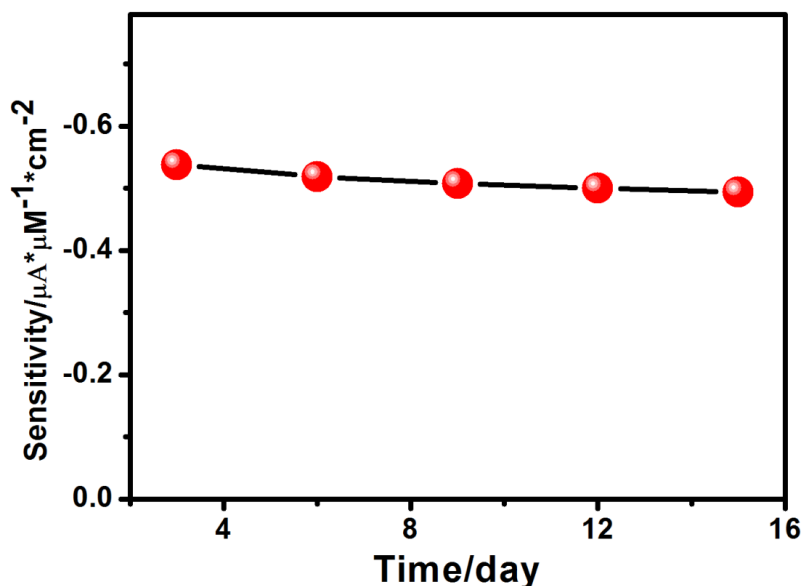


Figure 9. Stability of the AgNPs/MoS₂/GCE for sensitivity measurements to H₂O₂ tested for every three days.

The continuous long term stability testing was also carried out on the AgNPs/MoS₂-based H₂O₂ sensor for about 15 days. The amperometric measurements were performed on the as-prepared sensors for every 3 days and the changes in their sensitivity was evaluated, as shown in Fig.8. One can observed that the obtained sensitivity did not change much and still maintained about 94 % of its initial

sensitivity value even after 15 days of non-stop operation. All these results revealed that the developed AgNPs/MoS₂/GCE-based electrochemical sensor possesses good long-term ability for H₂O₂ detection.

3.5. Sample recovery test

Table 2. Determination of H₂O₂ in real samples.

Sample	H ₂ O ₂ added (mM)	H ₂ O ₂ found (mM)	Recovery (%)
1	1	0.97±0.04	97.0
2	2	1.95±0.05	97.5
3	5	5.02±0.05	100.4
4	10	10.1±0.10	101.0
5	20	20.5±0.15	102.5

To further evaluate the validity of the fabricated H₂O₂ sensor, amperometric response tests were carried out in known concentrations of H₂O₂ solution. Five samples were prepared with tap water using different amounts of H₂O₂, and the concentration of samples is 1, 2, 5, 10 and 20 mM. Then the amperometric experiments were carried out on as-prepared samples. Figure S2 (Supplementary Information) shows the chronoamperometric current responses which were performed by AgNPs/MoS₂/GCE sensor in the real samples. The results illustrates that the current can reach a steady value in a relatively short period of time. The test results are listed in Table 2. Those results demonstrated that the proposed H₂O₂ sensor can be used efficiently in real sample analysis.

4. CONCLUSIONS

Ag functionalized flower-like AgNPs/MoS₂ hybrid nanostructures were synthesized by simple hydrothermal method. All materials characterization techniques have confirmed their unique structure and morphology. Further electrochemical measurements have revealed that the AgNPs/MoS₂ hybrid nanostructured modified electrodes exhibited excellent catalytic activity, good selectivity and long-term stability for H₂O₂ detection, confirming that the development of functionalized hybrid nanostructured electrode with the high surface-to-volume ratio is indeed the substantially innovative approach towards the improvement of H₂O₂ sensing capabilities. Furthermore, compared with the other H₂O₂ sensors reported to date, the as-fabricated electrochemical H₂O₂ sensors shown a wide linear measured concentration range from 0.025 mM to 135.2 mM with lower detection limit of 3.5 μM. Thus, all presented experimental results appeared to indicate that the AgNPs/MoS₂ hybrid nanostructure is very promising sensor's electrode material for the robust and reliable H₂O₂ detection in many practical applications.

ACKNOWLEDGMENTS

This work was financially supported by the National Natural Science Foundation of China (51205274), Higher school science and technology innovation project of Shanxi (2016137, 2016138), Natural

Science of Shanxi Province (2016011039), Talent project of Shanxi Province (201605D211036), Science and Technology Major Project of the Shan Xi Science and Technology Department (20121101004), Key Disciplines Construction in Colleges and Universities of Shanxi ([2012]45).

SUPPLEMENTARY INFORMATION:

Table S1. The H₂O₂ dropping amount and current response of the seven experiments.

Dropping Times	I		II		III		IV	
	H ₂ O ₂ (mM)	Current (μA)	H ₂ O ₂ (mM)	Current (μA)	H ₂ O ₂ (mM)	Current (μA)	H ₂ O ₂ (mM)	Current (μA)
1	0.6	-6.566	0.6	-6.337	0.5	-6.156	0.6	-5.2955
2	1.2	-8.596	1.2	-8.009	1	-7.734	1.1	-6.3207
3	2.2	-13.445	1.8	-11.49	1.6	-10.555	1.6	-8.157
4	3.2	-17.757	2.8	-15.131	2.2	-13.39	1.9	-9.867
5	4.2	-21.584	3.8	-18.816	3.2	-16.64	2.2	-11.581
6	5.2	-25.679	4.8	-24.129	3.8	-19.789	3.2	-13.071
7	7.5	-36.758	6.8	-30.924	5.8	-27.365	4.2	-17.255
8	——	——	7.5	-38.755	7.5	-36.836	5.2	-21.807
9	——	——	——	——	——	——	7.5	-33.457
Dropping Times	V		VI		VII			
	H ₂ O ₂ (mM)	Current (μA)	H ₂ O ₂ (mM)	Current (μA)	H ₂ O ₂ (mM)	Current (μA)		
1	0.3	-5.0478	0.3	-4.931	0.3	-5.5943		
2	0.6	-6.2986	0.6	-5.913	0.6	-6.628		
3	1.1	-8.68	1.1	-8.199	0.9	-7.836		
4	1.6	-10.835	1.6	-10.795	1.2	-9.776		
5	2.1	-12.588	2.1	-12.731	1.5	-10.388		
6	2.6	-14.39	2.6	-14.791	2	-12.535		
7	3.8	-19.689	3.1	-16.599	2.5	-14.676		
8	5	-24.628	4.1	-20.362	3	-16.594		
9	6.2	-29.711	5.1	-25.021	3.5	-18.262		
10	7.5	-34.232	6.1	-29.229	4	-20.194		
11	——	——	6.7	-32.59	4.2	-21.801		
12	——	——	7.5	-36.503	4.6	-23.776		
13	——	——	——	——	5.6	-27.171		
14	——	——	——	——	6.6	-31.415		
15	——	——	——	——	7.5	-35.032		

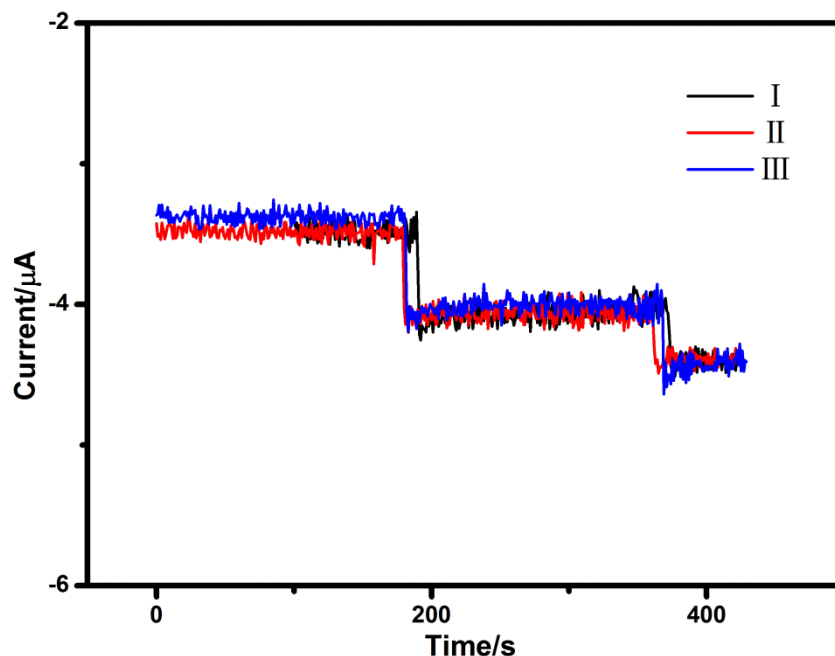


Figure S1. Interference study (three times) with the successive addition of 0.05 mM H₂O₂, 1.0 mM AA, 1.0 mM UA, 1.0 mM Glucose (Glu), 1.0 mM NO₃⁻, 1.0 mM NO₂⁻ and 0.05 mM H₂O₂ into a stirred N₂-saturated 0.2 M PBS (pH=6.5).

Fig. S1 presents three times of interference studies with the successive addition of interference in a stirred N₂-saturated 0.2 M PBS. Compared the four (including the results in the text) interference study results, we can find that there is only small difference among the results. Thus, the H₂O₂ sensor possesses excellence selectivity.

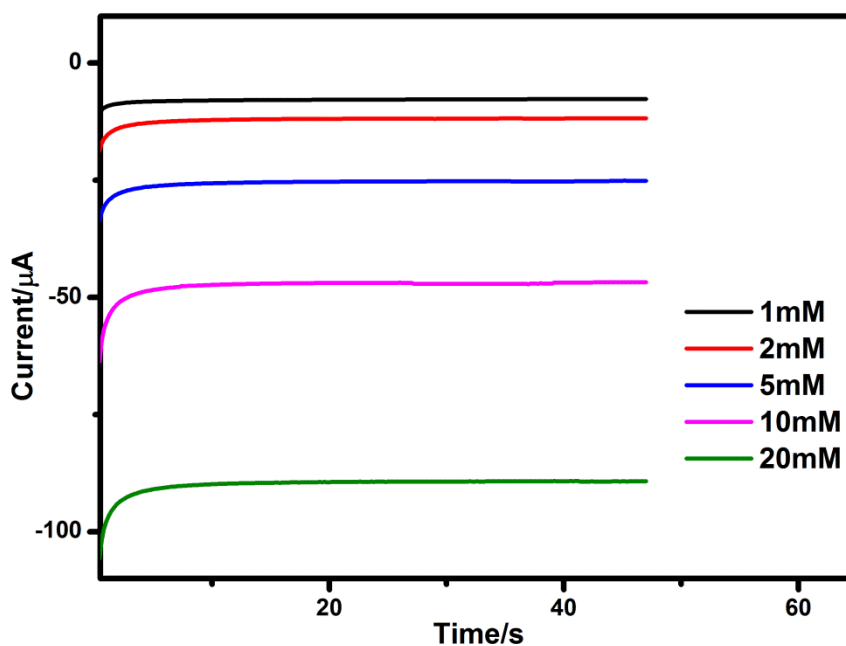


Figure S2. The amperometric response measurements for real samples

Amperometric experiments were carried out to determinate H₂O₂ in real samples. We prepared five H₂O₂ aqueous solutions with various concentrations of 1, 2, 5, 10 and 20 mM in tap water. Then, the prepared H₂O₂ sensor was used for detection of the prepared samples. Fig. S2 exhibits the amperometric responses results for real samples.

References

1. B.S. Lane, K. Burgess, *Chem. Rev.* 103 (2003) 2457.
2. Y. Tian, F. Wang, Y. Liu, F. Pang, X. Zhang, *Electrochim. Acta* 146 (2014) 646.
3. O. Sahin, H. Kivrak, A. Kivrak, H. Ç.Kazııcı, O. Alal, D. Atbas, *Int. J. Electrochem. Sci.* 12 (2017) 762.
4. H.L. Tan, C.J. Ma, Q. Li, L. Wang, F.G. Xu, S.H. Chen, Y.H. Song, *Analyst* 139 (2014) 5516.
5. Y. Liu, G.Z. Sun, C.B. Jiang, X.T. Zheng, L.X. Zheng, C.M. Li, *Microchim. Acta* 181 (2014) 63.
6. R. Bortolozzi, S.V. Gradowski, H. Ihmels, K. Schäfer, G. Viola, *Chem. Commun.* 50 (2014) 8242.
7. C. Chung, D. Srikun, C.S. Lim, C.J. Chang, B.R. Cho, *Chem. Commun.* 47 (2011) 9618.
8. L.J. Kong, Z.Y. Ren, N.N. Zheng, S.C. Du, J. Wu, J.L. Tang, H.G. Fu, *Nano Res.* 8 (2015) 469.
9. H.V. Tran, A.X. Trinh, C.D. Huynh, H.Q. Le, *Sens. Lett.* 14 (2016) 32.
10. Q.L. Zhang, D.L. Zhou, Y.F. Li, A.J. Wang, S.F. Qin, J.J. Feng, *Microchim. Acta* 181 (2014) 1239.
11. Y. Li, J.B. Zheng, Q.L. Sheng, B.N. Wang, *Microchim. Acta* 182 (2015) 61.
12. W. Zhao, H. Wang, X. Qin, X. Wang, Z. Zhao, Z. Miao, L. Chen, M. Shan, Y. Fang, Q. Chen, *Talanta* 80 (2009) 1029.
13. J.J. Jin, Y.Y. Ge, G.Y. Zheng, Y.P. Cai, W. Liu, G.H. Hui, *Food Chem.* 175 (2015) 485.
14. Y.H. Xu, X.X. Zhang, D.L. Chen, J.P. Hou, C. Li, X.L. Zhu, *Curr. Nanosci.* 9 (2013) 737.
15. X.Y. Qin, Q.Z. Li, A.M. Asiri, A.O. Al-Youbi, X.P. Sun, *Gold Bull.* 47 (2014) 3.
16. K.Y. Duan, Y.L. Du, Q.L. Feng, X.L. Ye, H. Xie, M.Y. Xue, C.M. Wang, *ChemCatChem* 6 (2014) 1873.
17. A.M. Golsheikh, N.M. Huang, H.N. Lim, R. Zakaria, C.Y. Yin, *Carbon* 62 (2013) 405.
18. W.B. Lu, F. Liao, Y.L. Luo, G.H. Chang, X.P. Sun, *Electrochim. Acta* 56 (2011) 2295.
19. C.M. Welch, C.E. Banks, A.O. Simm, R.G. Compton, *Anal. Bioanal. Chem.* 382 (2005) 12.
20. Y. Jiang, Y. Li, Y. Li, S. Li, *Anal. Methods* 8 (2016) 2448.
21. S. Liu, J.Q. Tian, L. Wang, X.P. Sun, *Carbon* 49 (2011) 3158.
22. J.Q. Tian, H.L. Li, W.B. Lu, Y.L. Luo, L. Wang, X.P. Sun, *Analyst* 136 (2011) 1806.
23. X.Y. Qin, W.B. Lu, Y.L. Luo, G.H. Chang, A.M. Asiri, A.O. Al-Youbi, X.P. Sun, *Electrochim. Acta* 74 (2012) 275.
24. D. Jiang, Y. Zhang, M. Huang, J. Liu, J. Wan, H. Chu, M. Chen, *J. Electroanal. Chem.* 728 (2014) 26.
25. X. Cui, G. Lee, Y.D. Kim, G. Arefe, P.Y. Huang, C. Lee, D.A. Chenet, X. Zhang, L. Wang, F. Ye, F. Pizzocchero, B.S. Jessen, K. Watanabe, T. Taniguchi, D.A. Muller, T. Low, P. Kim, J. Hone, *Nat. Nanotechnol.* 10 (2015) 534.
26. T.Y. Wang, H.C. Zhu, J.Q. Zhuo, Z.W. Zhu, P. Papakonstantinou, G. Lubarsky, J. Lin, M.X. Li, *Anal. Chem.* 85 (2013) 10289.
27. Y.P. Lin, X. Chen, Y.X. Lin, Q. Zhou, D.P. Tang, *Microchim. Acta* 182 (2015) 1803.
28. M. Govindasamy, V. Mani, S.M. Chen, R. Karthik, K. Manibalan, R. Umamaheswari, *Int. J. Electrochem. Sci.* 11 (2016) 2954.
29. S.X. Min, G.X. Lu, *J. Phy. Chem. C* 116 (2012) 25415.
30. H.L. Li, K. Yu, H. Fu, B.J. Guo, X. Lei, Z.Q. Zhu, *J. Phy. Chem. C* 119 (2015) 7959.
31. W.B. Lu, Y.L. Luo, G.H. Chang, X.P. Sun, *Biosens. Bioelectron.* 26 (2011) 4791.
32. L. Mattarozzi, S. Cattarin, N. Comisso, P. Guerriero, M. Musiani, E. Verlato, *Electrochim. Acta* 198 (2016) 296.

33. J.H. Lee, B. Huynh-Nguyen, E. Ko, J.H. Kim, G.H. Seong, *Sens. Actuators B* 224 (2016) 789.
34. Y. Zhang, Z. Wang, Y. Ji, S. Liu, T. Zhang, *RSC Adv.* 5 (2015) 39037.
35. W.B. Lu, F. Liao, Y.L. Luo, G.H. Chang, X.P. Sun, *Electrochim. Acta* 56 (2011) 2295.
36. M.R. Guascito, E. Filippo, C. Malitesta, D. Manno, A. Serra, A. Turco, *Biosens. Bioelectron.* 24 (2008) 1057.
37. A.M. Golsheikh, N.M. Huang, H.N. Lim, R. Zakaria, *RSC Adv.*, 2014, 4, 36401.
38. J.Q. Tian, H.L. Li, W.B. Lu, Y.L. Luo, L. Wang, X.P. Sun, *Analyst* 136 (2011) 1806.
39. W. Zhao, H.C. Wang, X. Qin, X.S. Wang, Z.X. Zhao, Z.Y. Miao, L.L. Chen, M.M. Shan, Y.X. Fang, Q. Chen, *Talanta* 80 (2009) 1029.
40. J. Zhang and J. Zheng, *Anal. Methods* 7 (2015) 1788.
41. B. Habibi, F.F. Azhar, J. Fakkar, Z. Rezvani, *Anal. Methods* 9 (2017) 1956.
42. S. Chairam, W. Sroysee, C. Boonchit, C. Kaewprom, T. G. N. Wangnoi, M. Amatatongchai, P. Jarujamrus, S. Tamaung, E. Somsook, *Int. J. Electrochem. Sci.* 10 (2015) 4611.

© 2017 The Authors. Published by ESG (www.electrochemsci.org). This article is an open access article distributed under the terms and conditions of the Creative Commons Attribution license (<http://creativecommons.org/licenses/by/4.0/>).